China Geology 9 (2026) 86−101

China Geology

Journal homepage: http://chinageology.cgs.cn
https://www.sciencedirect.com/journal/china-geology

Geochemistry, possible origin and exploration potential of crude oils from Neogene Shawan Formation in the Chepaizi Uplift, Junggar Basin (NW China) based on biomarker recovery method

Chen-yu Wang[a], Xiang-chun Chang[a, b,*], You-de Xu[c], Bing-bing Shi[a], Tian-chen Ge[a], Wei-zheng Gao[a], Lei Su[a]

[a] *College of Earth Science and Engineering, Shandong University of Science and Technology, Qingdao* 266590, *China*
[b] *Laboratory for Marine Mineral Resources, Qingdao Marine Science and Technology Center, Qingdao* 266237, *China*
[c] *Research Institute of Petroleum Exploration and Development, Shengli Oilfield Company, Sinopec, Dongying* 257015, *China*

A R T I C L E I N F O

Article history:
Received 29 February 2024
Received in revised form 21 August 2024
Accepted 24 August 2024
Available online 24 June 2025

Keywords:
Biomarker recovery
Oil-source correlation
Stable carbon isotope
Heavy and light oil identify
Oil-gas exploration potential
Chepaizi Uplift
Neogene Shawan Formation
Petroleum exploration engineering
Junggar Basin.

A B S T R A C T

The Neogene Shawan Formation in the Chepaizi Uplift of the Junggar Basin (NW China) has obtained high oil flow, demonstrating a good potential for oil and gas exploration. The multi-source hydrocarbon generation background and strong tectonic activity have led to the simultaneous production of heavy oil and light oil from multi-layer in the area, which makes it very difficult to identify oil origins, presently, the hot debate on the oil origins needs to be clarified. In this paper, due to the selective consumption of different types of compounds in crude oils by severe and intense biodegradation, the commonly used oil-source correlation tools are ineffective or may produce misleading results, this study adopted a biomarker recovery method based on the principle of mass conservation that uses the sum of the mass of the residual biomarkers and their corresponding biodegradation products to obtain the mass of the original biomarkers, improving the reliability of oil origins determination. Based on the nature and occurrence of crude oils, the investigated oils are subdivided into three types, Group A, Group B and Group C. Group A, light oils occurred mainly in lower structure Neogene Shawan Formation in the western Chepaizi Uplift, while Group B, heavy oils occurred mainly in higher structure Neogene Shawan Formation in the western Chepaizi Uplift. The two types of crude oils may come from the mixed source of Jurassic Badaowan Formation source rocks (J_1b) and Paleogene Anjihaihe Formation source rocks ($E_{2\text{-}3}a$) in the Sikeshu Sag, and Jurassic Badaowan Formation source rocks (J_1b) are the main source of crude oils. Group C, heavy oils occurred mainly in Neogene Shawan Formation in the eastern Chepaizi Uplift, showing good correlation with the Permian (P_1f and P_2w) source rocks in the Shawan Sag. At the same time, by combining stable carbon isotope and parameters related to triaromatic steroids, the accuracy of the oil-source correlation results by biomarker recovery method was further verified.

©2026 China Geology Editorial Office.

1. Introduction

The Chepaizi Uplift is located at the southern part of the northwest margin of Junggar Basin, adjacent to Shawan Sag in the east, Sikeshu Sag in the south, and Mount Zaire in the west and north (Jin X et al., 2007; Zhang ZH et al., 2007; Dong DW et al., 2015; Wang K et al., 2017; Chang XC et al., 2019; Li Y et al., 2021). Billions of tons of oil and gas reserves have been discovered in Neogene Shawan Formation (Dong YL et al., 2017; Zhao XD et al., 2021), which shows a good oil-gas prospect.

At present, the exploration practices show that the crude oils properties in this area are relatively complex, both light oils and heavy oils were found with greatly changed physical properties, which makes the determination of oil origins very difficult. The oil origins for the Neogene Shawan Formation in the Chepaizi Uplift have become a controversial issue.

Several scholars have conducted in-depth analysis and research on the oil origins of this layer from the perspective of geochemical methods based on the characteristics of biomarkers in crude oils, achieving some important results and understanding, but there are still some controversies. The main viewpoints on the source of Neogene Shawan Formation heavy oil in the Chepaizi Uplift include the mixed source of

First author: *E-mail address*: 824127348@qq.com (Chen-yu Wang).

* Corresponding author: *E-mail address*: xcchang@sdust.edu.cn (Xiang-Chun Chang).

Literary editor: Li-qiong Jia
doi:10.31035/cg2024022
2096-5192/© 2026 China Geology Editorial Office.

Copyright © 2026 Editorial Office of China Geology. Publishing services by Elsevier B.V. on behalf of KeAi Communications Co. Ltd.
This is an open access article under the CC BY-NC-ND License (http://creativecommons.org/licenses/by-nc-nd/4.0/).

Permian source rocks in the Shawan Sag and Jurassic source rocks in the Sikeshu Sag (Xi WJ et al., 2014; Zhang ZH et al., 2014; Li ET et al., 2021), as well as the single source of Permian source rocks in the Shawan Sag (Ren YZ, 2014). For the source of Neogene Shawan Formation light oil in the Chepaizi Uplift, there are six viewpoints: (1) The single source of Jurassic Badaowan Formation (J_1b) source rocks in the Sikeshu Sag (Li Z et al., 2011; Li ET et al., 2021); (2) the primary source of Jurassic Badaowan Formation (J_1b) source rocks is mixed with Cretaceous source rocks in the Sikeshu Sag (Liu HJ et al., 2011; Liu ZQ et al., 2022; Zhang ZY et al., 2020); (3) the primary source of Jurassic Badaowan Formation (J_1b) source rocks is mixed with Paleogene Anjihaihe Formation ($E_{2\text{-}3}a$) source rocks in the Sikeshu Sag(You WF and Meng XL, 2006; Yang PC et al., 2015); (4) the primary source of Jurassic Badaowan Formation (J_1b) source rocks in the Sikeshu Sag is mixed with Permian source rocks in the Shawan Sag(Zhang WL et al., 2003); (5) primarily originated from the highly matured Permian source rocks in the neighboring Shawan Sag (Zhang XJ et al., 2013), (6) primarily originated from Paleogene Anjihaihe Formation ($E_{2\text{-}3}a$) source rocks in the Sikeshu Sag (Wang QJ et al., 2020). Previous oil origins studies were mainly based on the molecular biomarker parameters, however, some biomarkercompounds are greatly influenced by post-accumulation alteration, especially biodegradation. Thus, commonly used oil-source correlation tools, such as bivariate cross plots of biomarker parameters cannot effectively distinguish oil origins (Song FQ et al., 2004; Curiale JA, 2008).

Biomarker recovery method is proved to address this problem (Chang XC et al., 2022; Wang ZY et al., 2023). Biomarker recovery method is based on the formation mechanism of biomarkers and the principle of mass conservation, using the sum of the mass of the residual biomarkers and their corresponding degradation products to obtain the mass of the original biomarkers. It can restore the original biomarker characteristics of crude oils, making it possible to determine the source of crude oils using traditional and important biomarker parameters.

Stable carbon isotope can reflect the source of compounds at the molecular level, the distribution mainly depends on the original sedimentary environment of the parent rocks and the input of biogenic sources, and is relatively less affected by biodegradation, and other factors (Liu HL et al., 2004).

This study attempted to define the populations of crude oils by hierarchical cluster analysis (HCA) and then combined with the biomarker recovery method to determine oil origin. In addition, biomarker parameters that are still valid under severe biodegradation and stable carbon isotope ($\delta^{13}C$) were combined to confirm their validity. This method can improve the reliability of oil-source correlation, which is conducive to the in-depth exploration of oil.

2. Geological setting

2.1. Regional geological overview

The Junggar Basin is located in the northern part of Xinjiang, China. It is a large oil and gas superposition basin, which develops multiple sets of hydrocarbon source rocks in varying degrees, such as Carboniferous, Permian, Triassic, Jurassic and Paleogene, and its petroleum geological conditions are relatively favorable. The Chepaizi Uplift is located at the southern part of the northwest margin of Junggar Basin, and belongs to the second-order tectonic unit of the uplift in the western part of the basin. The Chepaizi Uplift is adjacent to Shawan Sag in the east, Sikeshu Sag in the south, and Mount Zaire in the west and north (Fig. 1).

2.2. Tectonic evolution history

It is an ancient uplift formed in the Late Hercynian period, and has been inherited and developed for a long time (Zhuang XM, 2009), and its tectonic evolution can be divided into four stages. The first stage is from the Late Hercynian to the Middle Yanshanian (Carboniferous–Jurassic), strong uplift formed the Hongche Fault Zone and led to the lack of Permian–Cretaceous deposits in the study area. The second stage is from the Late Yanshanian to the Early Himalayan (Early Cretaceous–Eocene), and the Chepaizi Uplift has undergone a long-term southward adjustment. The third and fourth stages refer to a span of time after Paleogene, when slow subsidence and rapid subsidence led to thick deposits of Neogene Shawan Formation, Taxihe Formation and Dushanzi Formation in Chepaizi Uplift (Xiao F et al., 2015).

2.3. Stratigraphic development

The uplift developed Cretaceous, Paleogene, Neogene, and Quaternary from bottom to top. The Neogene developed the Shawan Formation, Taxihe Formation, and Dushanzi Formation from bottom to top. With a basic lack of Permian, Triassic, and Jurassic strata, it is directly overlaid and deposited on the top of Carboniferous bedrock (Wang K et al., 2017).

2.4. Petroleum geological conditions

Since Neogene under the influence of Himalayan Neotectonic activities, the Chepaizi Uplift has tilted locally and received Neogene deposition. After Neogene deposition, the tectonic movement was obviously strengthened, and large-scale faults developed, resulting in Neogene oil and gas accumulation. The Chepaizi Uplift is close to the two hydrocarbon generating centers of Sikeshu Sag and Shawan Sag, and has multiple sets of potential hydrocarbon source rocks, which provides favorable oil origins conditions for the study area. It is precisely because of the development of many hydrocarbon-generating Sags and multiple sets of source rocks around this area that the oil origins of Neogene Shawan Formation in the Chepaizi Uplift are very complicated (Fig. 1).

3. Experimental section

3.1. Sample preparation

The samples for this study were obtained from 23

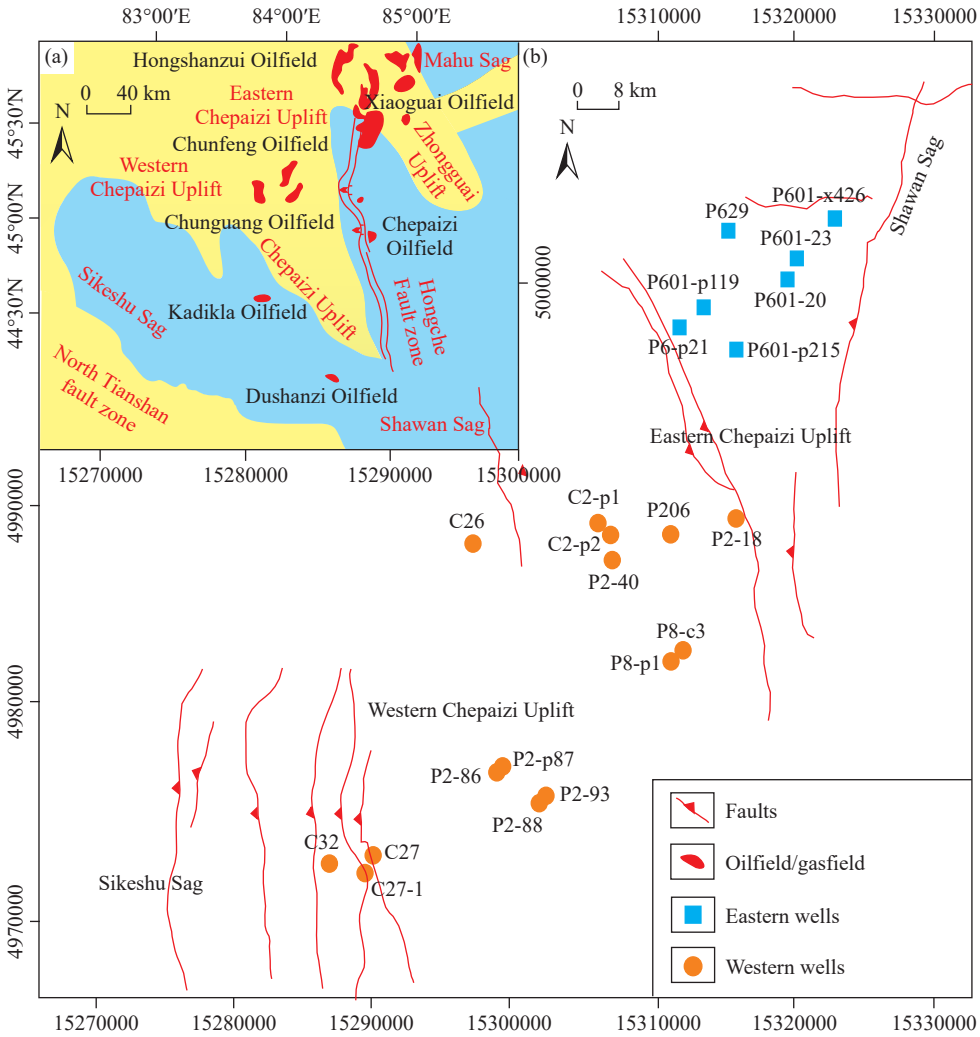

Fig. 1. a–Structural position of Chepaizi Uplift; b–Neogene Shawan Formation well location of eastern and western Chepaizi Uplift.

Neogene reservoir rock samples from the eastern and western Chepaizi Uplift, including 7 samples from the eastern Chepaizi Uplift and 16 samples from the western Chepaizi Uplift. Additionally, 14 source rock samples were also collected for geochemical analysis. The pretreatment steps are as follows: First, the samples were pulverized to less than 100 mesh by GJ series sealing crusher; then, LabTech high-speed solvent extraction (HPSE) instrument was used to extract saturated hydrocarbon and aromatic hydrocarbon from the crushed samples. Finally, the saturated hydrocarbon and aromatic hydrocarbon were separated by column chromatography, and then the extraction liquid was transferred to the alumina-silica gel column, and the saturated hydrocarbon and aromatic hydrocarbon were eluted by the mixed solution of n-hexane and dichloromethane (2∶1, v∶v), and the volatile reagents were put into the chromatographic bottle for testing.

3.2. Experimental analysis

3.2.1. Gas chromatography–Mass spectrometry (GC–MS) method

Following regulations in *Organic Geochemical Analysis Methods for Geological Samples–Part5*: *Analysis of Saturated Hydrocarbons in Rock Extracts and Crude Oils–Gas Chromatography* (GB/T 18340.5–2010) and the *Test Method for Biomarkers in Sediment and Crude Oil by GC–MS* (GB/T 18606–2017). Instruments used: Agilent 7890A chromatograph, Agilent 5975C mass spectrometer. The chromatographic column was HP-5 elastic quartz capillary column (30 m×0.25 mm×0.25 μm). Test conditions: 99.999% He. The GC oven temperature for analysis of the saturate fractions was initially held at 50°C for 1 min, maintained for 1 min, and then the temperature was raised to 310°C at 3°C/min and kept for 15 min. The GC oven temperature for analysis of the aromatic fractions was initially held at 80°C for 1 min before being programmed to 310°C at 3°C/min and held at 310°C for 16 min. The flow rate of helium gas was 1 mL/min. The split injection was 1 μl, the diversion ratio was 10∶1.

3.2.2. Stable carbon isotope analysis

Following regulations in *Organic Geochemical Analysis Method for Geological Samples–Part2: Determination of Organic Carbon Stable Isotopic Component–Isotopic Mass Spectrometry* (GB/T 18340.2–2010). Instruments used: Finnigan MAT-252 Delta Plus MS combined instrument. Test

condition: 99.999% He. The carrier gas flow rate was 100 mL/min. The combustion gas was high-purity oxygen. The reactor temperature was 980°C. The reactor packing was chromium oxide, reduced copper and silver containing cobalt oxide, filling column temperature was 50°C. MAT-253 Mass spectrum: EI source with an ionization voltage of 70 eV.

4. Results and discussion

4.1. Geochemical characteristics of Neogene crude oils

4.1.1. Physical characteristics of Neogene crude oils

Crude oils present different physical characteristics, which can reflect the differences in the original oil-generating parent material types, degree of thermal evolution, and secondary changes of reservoir formation during the geological historical period (Shi BB et al., 2019). The physical properties of different crude oils are mainly reflected in their density, viscosity, freezing point, wax content, and sulfur content. Previous investigations have shown that great changes have taken place in the physical properties of Carboniferous crude oils in the Chepaizi Uplift, which is due to the severe and intense biodegradation of crude oils from the eastern Chepaizi Uplift (Chang XC et al., 2018, 2019, 2022).

As shown in Table 1, the Neogene crude oils from the western Chepaizi Uplift exhibit a relatively wide density range (0.820 g/cm^3 to 0.917 g/cm^3), and about 50% of those crude oils are light oil. However, the oils from Wells C26, C2-p1, C2-p2, P2-88, and P2-93 near the eastern Chepaizi Uplift show characteristics of medium oil (0.889 g/cm^3 to 0.901 g/cm^3), with a viscosity ranging from 1.78 MPa·s to 22.77 MPa·s. The Neogene crude oils from the eastern Chepaizi Uplift show the characteristics of heavy super-heavy oil (0.942 g/cm^3 to 1.067 g/cm^3), and high-viscosity oil (360 MPa·s to 6392 MPa·s). The density (0.926 g/cm^3 to 0.9648 g/cm^3) and viscosity (154 MPa·s to 8388 MPa·s) range of Carboniferous crude oils from the eastern Chepaizi Uplift are similar to that of Neogene crude oils from the eastern Chepaizi Uplift (Shi BB et al., 2019, 2020b; Mao LX et al., 2020; Chang XC et al., 2022), which indicate that possible severe and intense biodegradation also occurred. In addition, the viscosity of crude oils increases exponentially with the increase of density in an overall exponential positive correlation (Fig. 2). The density and viscosity of Neogene Shawan Formation crude oils in the Chepaizi Uplift also show a certain negative correlation with their corresponding depth, that is, with the increase of burial depth, the density and viscosity of crude oils decrease, reflecting that a certain influence of secondary effects on crude oils composition (Fig. 3).

4.1.2. Composition characteristics of Neogene crude oil populations

The bulk composition and triangular diagram of Neogene crude oils in the Chepaizi Uplift (Table 1; Fig. 4) show that the total hydrocarbons of crude oils from the western Chepaizi Uplift is high (43.70%–91.90%, average 79.18%), and the relative proportion of saturated hydrocarbon is high (32.10%–78.32%, average 61.18%). The content of non-hydrocarbon and asphaltene is relatively low (8.10%–42.70%, average 20.89%), and saturated/aromatic ratio is high

Table 1. Physical characteristics of Neogene Shawan Formation crude oils in the Chepaizi Uplift.

Position	Well	Depth /m	Density /(g/cm^3)	Viscosity /MPa·s	Saturated hydrocarbon /%	Aromatics /%	Non-hydrocarbon and asphaltene /%	Saturated/ Aromatic	Total hydrocarbon/%
Western Chepaizi Uplift	C26	997.20	0.889	/	56.09	18.56	25.35	3.02	74.65
	C27	1295.59	0.820	2.79	71.66	14.40	13.94	4.98	86.06
	C27-1	1621.31	0.840	5.94	/	/	/	/	/
	C2-p1	1273.00	0.917	30.00	67.70	17.4	14.9	3.89	85.1
	C2-p2	1077.00	0.936	31.00	39.33	34.14	26.53	1.15	74.47
	C2-p41	1096.00	0.876	/	76.39	13.77	9.84	5.55	90.16
	C32	1634.30	0.820	4.63	/	/	/	/	/
	P206	989.20	0.814	1.78	77.67	13.02	9.31	5.97	90.69
	P2-18	981.60	0.800	1.39	76.90	15.00	8.10	5.13	91.90
	P2-40	1003.00	0.814	2.19	78.32	9.14	12.54	6.49	87.46
	P2-86	1391.90	0.858	11.91	37.00	6.70	56.30	5.52	43.70
	P2-88	1401.10	0.896	17.75	52.00	5.30	42.70	9.81	57.30
	P2-93	1396.00	0.901	22.77	38.56	19.47	41.97	1.98	58.03
	P2-p87	1505.00	0.857	12.90	32.10	54.60	13.30	0.59	86.70
	P8-c3	1195.20	0.833	3.37	75.84	14.75	9.41	5.14	90.59
	P8-p1	1360.00	0.828	3.37	76.95	14.77	8.28	5.21	91.72
Eastern Chepaizi Uplift	P601-p215	436.00	0.947	360.00	58.60	27.60	13.80	2.12	86.20
	P601-20	442.00	0.942	2494.00	/	/	/	/	/
	P601-23	413.40	0.978	/	/	/	/	/	/
	P601-p119	436.00	0.947	3060.00	24.80	12.70	62.50	1.95	37.50
	P601-x426	463.00	0.980	3100.00	51.04	18.15	30.81	2.81	69.19
	P629	405.00	0.989	/	12.96	26.13	60.91	0.50	39.09
	P6-p21	398.90	1.067	6392.00	48.48	22.96	28.56	2.11	71.44

(0.59–9.81, average 4.60), indicating that the degree of biological secondary modification of crude oils in the region is relatively light. The saturated hydrocarbon of Neogene crude oils from the eastern Chepaizi Uplift decreased (12.96%–58.60%, average 39.18%) compared with that of crude oils from the western Chepaizi Uplift, and the content of non-hydrocarbon and asphaltene increased (13.80%–62.50%, average 39.32%) compared with crude oils from the western Chepaizi Uplift. It has a low saturates/aromatic ratio (0.5–2.81, average 1.90), indicating that the crude oil populations' components have different characteristics in different structural units.

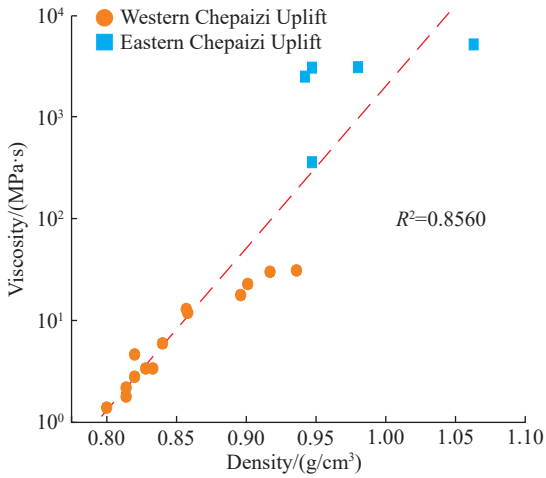

Fig. 2. Correlation plot between density and viscosity of Neogene crude oils in the Chepaizi Uplift.

4.2. Hierarchical Cluster Analysis to define Neogene crude oil populations

The crude oils from the same source rocks or oil origin areas are defined as the same crude oil populations, that is, the oils from the same populations have similar organic facies, reflecting the source rocks' input, hydrocarbon generation parent material, and sedimentary environment are consistent. Hierarchical Cluster Analysis (HCA) is a common statistical method, which is an effective tool for defining oil populations and oil-source correlation (Shi BB et al., 2019, 2020a).

Among them, HCA adopts the Wald method to calculate the similar distance of samples according to the similar distance of variables and divide samples into different groups (Shi BB et al., 2020a). The previous investigations found that the crude oils in the Chepaizi area generally suffered severe and intense biodegradation, and their physical and chemical

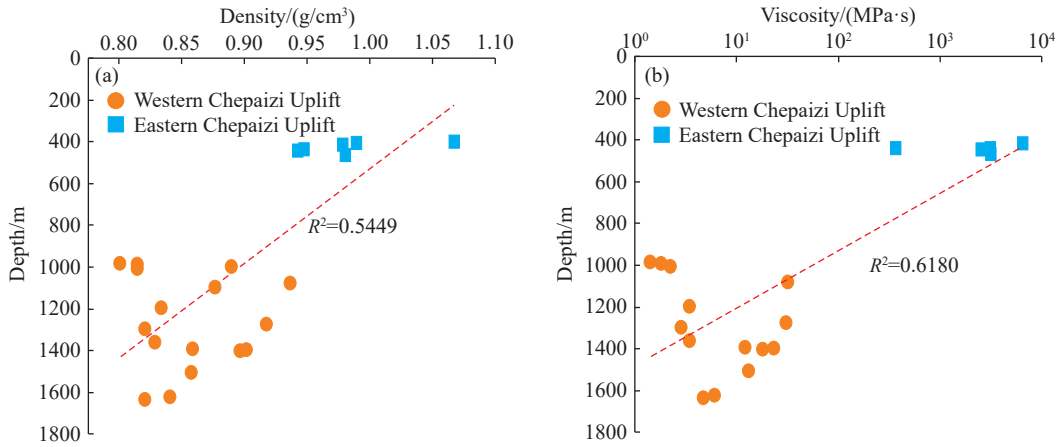

Fig. 3. a–Correlation plots between density and depth of Neogene crude oils in the Chepaizi Uplift; b–correlation plots between viscosity and depth of Neogene crude oils in the Chepaizi Uplift.

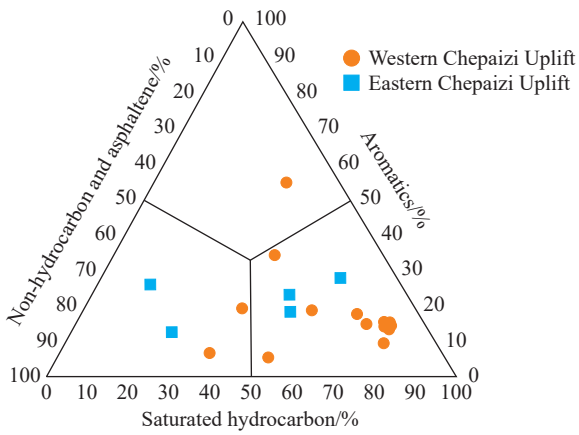

Fig. 4. Tri-diagram of Neogene crude oil populations in the Chepaizi Uplift.

properties changed greatly (Zhang ZH et al., 2014; Chang XC et al., 2018; Xu YD et al., 2018; Liu ZQ et al., 2022). Tricyclic terpanes, tetracyclic terpanes, and triaromatic steroids are not particularly sensitive to biodegradation, they do not completely change at PM<10 and are commonly used as indicators for defining oil populations (Peters KE and Moldowan JM, 1993), and these parameters can reflect the sedimentary environment. Therefore, seven geochemical parameters related to tricyclic terpanes (TT), tetracyclic terpanes (Tet) and triaromatic steroids (TAS), which are highly resistant to biodegradation and can reflect the source of parent material and sedimentary environment, as well as stable carbon isotope values of whole oil are selected: $(C_{19}TT+C_{20}TT)/(C_{23}TT+C_{24}TT)$, $C_{23}TT/C_{21}TT$, $C_{24}TT/C_{23}TT$, ETR, $C_{24}Tet/C_{26}TT$, $C_{26}TAS/C_{28}TAS(20S)$, $C_{27}TAS/C_{28}TAS(20R)$, $\delta^{13}C$.

The cluster pedigree diagram (Fig. 5; Table 2) shows that the Neogene crude oils in the Chepaizi Uplift can be divided into three groups (A, B, and C) according to their similarity.

4.3. PM evaluation biodegradation

Peters KE and Moldowan JM (1993) established a scale for evaluating biodegradation (named PM scale) based on the resistance of compound types to microbial erosion. Wenger LM et al. (2002) also added explanations based on the appearance or absence of certain important compounds, or the degree of intrinsic alteration of certain compounds, and stipulated that light=PM1–3, moderate=PM4–5, severe=PM6–7, very severe=PM8–9, extreme=PM10.

The TIC chromatogram baseline shows a distinct "bulge",

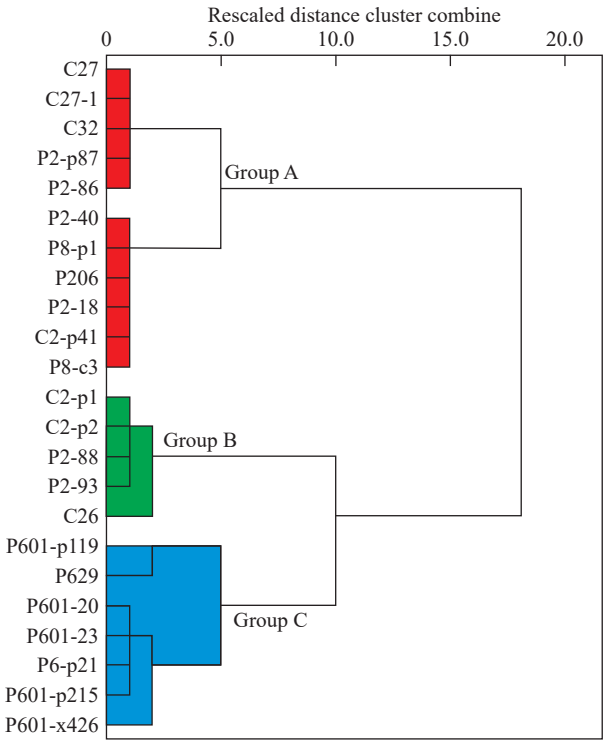

Fig. 5. Neogene crude oil populations defined in the Chepaizi Uplift by Hierarchical Cluster Analysis(HCA).

reflecting complex mixtures that are not resolved by chromatographic analysis, known as UCM peaks, which are often used as a sign of biodegradation of crude oils (Guo MY et al., 2018). Short-chain n-alkanes (C_{22}^{-}) are preferentially removed in the earliest stages of biodegradation compared to long-chain n-alkanes (PM<2, Peters KE and Moldowan JM, 1993). The ratios of $(nC_{21}+nC_{22})/(nC_{28}+nC_{29})$ of crude oils can be used to reflect the biodegradation level in the earliest stages. In previous studies, the ratio of TeMN (TeBR=1, 3, 6, 7-TeMN/1, 3, 5, 7-TeMN) can be used to characterize the loss of polycyclic aromatic hydrocarbon isomers at PM5–6 (Peters KE and Moldowan JM, 1993). Previous studies have indicated that C_{29} 25-norhopane (25-NH) is a degradation product of C_{30} hopane ($C_{30}H$) (PM⩾6, Li NX et al., 2015), and the high abundance of 25-NH is a result of severe biodegradation. Regular sterane (RS) takes priority over diasterane (DS) for degradation, C_{27}, C_{28}, C_{29} regular sterane take priority over C_{20}, and C_{21} regular sterane undergo degradation (PM⩾6, Peters KE and Moldowan JM, 1993). Tricyclic terpane (TT) can resist biodegradation at least PM8, 17-nortricyclic terpane (17-NT) is formed by demethylation of tricyclic terpane, which is similar to the mechanism of producing 25-NH from hopane (Cheng X et al., 2016). Extensive researches have shown that triaromatic steroids (TAS) can resist biodegradation at PM10 (Zhang BS et al., 2016), and short-chain C_{20}–$C_{21}TAS$ is more easily biodegradable than long-chain C_{26}–$C_{28}TAS$. Therefore, the values of $C_{20}/C_{28}TAS$ and $C_{21}/C_{28}TAS$ decrease with the increase of biodegradation level. Based on the analysis of total ion chromatograms of saturated hydrocarbon, *m/z* 191, *m/z* 217, *m/z* 231 mass chromatograms and biomarker parameters found that the crude oils in the Chepaizi Uplift exhibited different biodegradation characteristics, and the corresponding biodegradation level of crude oils in the Chepaizi Uplift were evaluated.

Group A crude oils are mainly located in the relatively low structural position from the western Chepaizi Uplift, and the TIC chromatograms of saturated hydrocarbon show that normal alkanes are still relatively complete, the ratios of $(nC_{21}+nC_{22})/(nC_{28}+nC_{29})$ are relatively high (2.43–5.21, average 3.57). The distribution of hopanes in *m/z* 191 chromatograms are relatively complete and C_{30} hopane is the peak compound. The ratios of C_{29} 25-NH/$C_{30}H$ are less than 0.1 (0.01–0.32, average 0.09), the abundance of tricyclic terpanes are much lower than that of hopanes, and the ratios of C_{22} 17-NT/$C_{23}TT$ are less than 0.01 (0.03–0.08, average 0.06). The regular steranes in *m/z* 217 chromatograms are abundant in content. The relative abundance of pregnane and homopregnane are much lower than that of regular steranes, and the content of diasteranes are relatively low. Among the regular sterane isomers, ααα20R is still the peak one, the ratios of $C_{27}DS/C_{29}RS$ show a lower range of 0.16–0.31 (average 0.24). However, in *m/z* 231 chromatograms, phenanthrenes and naphthalenes are relatively intact, the distribution of triaromatic steroids are intact, the content of $C_{20–21}$ triaromatic steroids are relatively high, and the ratios of

Table 2. Oil populations defined of Neogene Shawan Formation in the Chepaizi Uplift.

Position	Well	C_{26} TAS/ C_{28} TAS(20S)	C_{27} TAS/ C_{28} TAS(20R)	C_{24} Tet/ C_{26} TT	C_{24} TT/ C_{23} TT	(C_{19} TT+C_{20} TT)/ (C_{23} TT+C_{24} TT)	C_{23} TT/ C_{21} TT	δ^{13}C/‰	*ETR* (Equivalent Thermal Maturity)
Group A	C27	0.50	0.63	1.58	0.84	1.39	1.05	−27.40	0.53
	C27-1	0.51	0.62	1.49	0.76	1.32	1.20	−27.40	0.56
	C2-p41	0.51	0.70	2.29	0.80	2.57	1.03	−26.70	0.50
	C32	0.52	0.63	1.50	0.75	1.46	1.13	−27.80	0.49
	P206	0.52	0.60	2.34	0.85	3.06	1.07	−26.80	0.41
	P2-18	0.53	0.68	2.04	0.81	3.26	0.98	−26.80	0.44
	P2-40	0.59	0.66	1.90	1.00	3.34	0.90	−26.80	0.50
	P2-86	0.47	0.66	1.17	0.96	1.2	0.94	−27.80	0.46
	P2-p87	0.50	0.64	1.51	0.88	1.14	1.01	−28.10	0.51
	P8-c3	0.49	0.64	2.59	0.92	3.33	0.98	−26.60	0.52
	P8-p1	0.50	0.69	2.08	1.03	3.13	0.83	−27.10	0.52
Group B	C26	0.29	0.49	2.34	0.61	2.06	0.97	−27.00	0.48
	C2-p1	0.19	0.54	0.94	0.50	1.26	0.95	−28.30	0.55
	C2-p2	0.17	0.47	1.07	0.55	1.24	0.96	−28.80	0.55
	P2-88	0.16	0.46	1.23	0.51	1.28	0.95	−27.30	0.40
	P2-93	0.17	0.43	1.28	0.55	1.35	0.91	−27.80	0.47
Group C	P601-p215	0.16	0.62	0.48	0.37	0.52	1.80	−30.50	0.58
	P601-20	0.15	0.82	0.51	0.39	0.49	1.00	−30.90	0.50
	P601-23	0.12	0.77	0.46	0.39	0.92	0.77	−30.90	0.56
	P601-p119	0.13	0.77	0.46	0.87	0.65	3.7	−30.50	0.54
	P601-x426	0.51	0.69	0.48	0.35	0.52	0.96	−30.50	0.58
	P629	0.14	0.63	0.46	0.94	0.77	2.09	−30.30	0.69
	P6-p21	0.16	0.61	0.59	0.40	0.98	0.91	−30.40	0.60

Note: *ETR*=(C_{28} TT+C_{29} TT)/C_{26} TT.

C_{20-21}TAS/C_{28}TAS remain unchanged. All the above indicate that the biodegradation level of crude oils in this region are in the stage of light to moderate (PM<5) (Figs. 6a–d; Table 3).

Group B crude oils are mainly located in the relatively high structural position from the western Chepaizi Uplift, and the TIC chromatograms of saturated hydrocarbon have shown an obvious UCM bulge, the ratios of (nC_{21}+nC_{22})/(nC_{28}+nC_{29}) decreases relative to Group A crude oils (1.77–3.27, average 2.43). In *m/z* 191 chromatograms, hopanes have been depleted, the relative abundance of 25-NH have increased, and the ratios of C_{29} 25-NH/C_{30}H are between 0.12 and 0.42 (average 0.32). The abundance of tricyclic terpanes are much lower than that of hopanes, and the ratios of C_{22} 17-NT/C_{23}TT are between 0.04 and 0.06 (average 0.05). In *m/z* 217 chromatograms, regular steranes have substantial depletion, the relative abundance of pregnane and homopregnane are slightly lower than that of regular steranes, and the content of diasteranes are relatively low. Among the regular sterane isomers, ααα20S is the peak one, the ratios of C_{27}DS/C_{29}RS show a lower range of 0.28–0.56 (average 0.38). In *m/z* 231 chromatograms, phenanthrenes and naphthalenes are relatively complete, the content of C_{20-21} triaromatic steroids are high, and the ratios of C_{20-21}TAS/C_{28}TAS remain unchanged. The biodegradation level of crude oils in this region are higher than that of Group A crude oils, and have reached the stage of moderate to severe (5<PM<7) (Figs. 6e–f; Table 3).

Group C crude oils are mainly located in the eastern Chepaizi Uplift, the TIC chromatograms of saturated hydrocarbon show a significant UCM bulge, and it is difficult to detect distinguishable n-alkanes. In *m/z* 191 chromatograms, hopanes are lost, gammacerane and relatively high (0.10–1.60, average 0.79), 25-NH can be seen, the ratios of C_{29} 25-NH/C_{30}H are between 2.21 and 16.57 (average 4.30), the abundance of tricyclic terpanes are basically the same as that of hopanes, and C_{23} tricyclic terpanes have also undergone a substantial loss. The ratios of C_{23}TT/C_{30}H begin to decrease, and the ratios of C_{22} 17-NT/C_{23}TT are around 1.0 (0.19–1.38, average 0.69). In *m/z* 217 chromatograms, regular steranes have been basically depleted, and the relative abundance of pregnane and homopregnane are much higher than that of regular steranes, and diasterane is the peak one, the ratios of C_{27}DS/C_{29}RS show a lower range of 0.24–0.73 (average 0.52). In *m/z* 231 chromatograms, phenanthrenes and naphthalenes are basically lost, C_{20-21} triaromatic steroids are basically consumed, and the ratios of C_{20-21}TAS/C_{28}TAS begin to decrease, which generally indicate that the biodegradation level of crude oils in this area is the highest, and has reached the stage of very severe to extreme (PM>8+) (Figs. 6g–h; Table 3).

The scatter plots using the parameters indicating the biodegradation level also showed that the biodegradation level of Group A and Group B to Group C crude oils gradually increased (Fig. 7).

In summary, the biodegradation level of crude oils from Group A, Group B and Group C are roughly bounded by PM7, while crude oils range from lightly biodegraded PM1 to extremely biodegraded PM9+. Overall, the loss of various

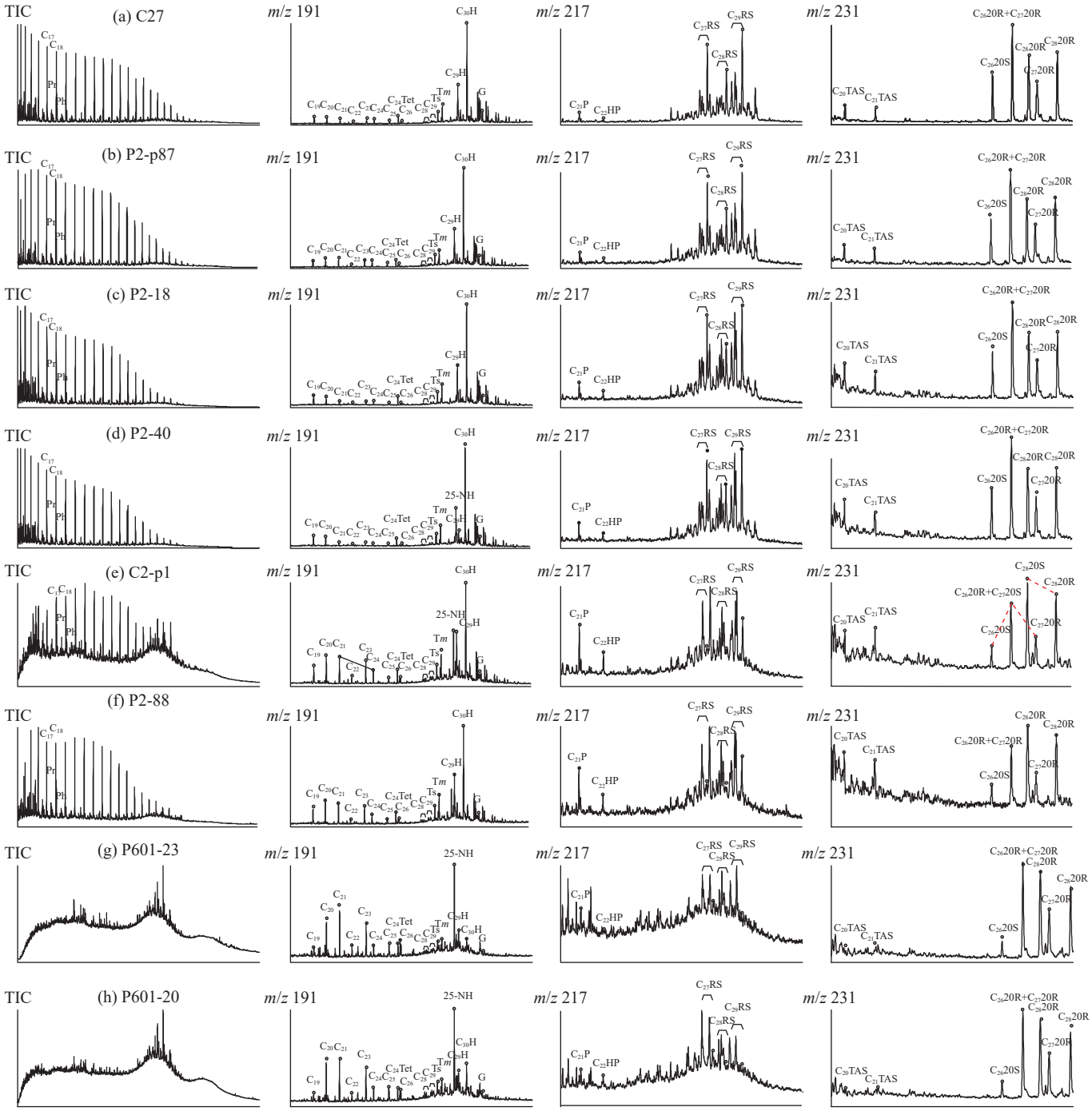

Fig. 6. Mass chromatograms of TIC, *m/z* 191, *m/z* 217 and *m/z* 231 crude oils from Neogene Shawan Formation. Pr–pristane; Ph–phytane; H–hopane; NH–norhopane; Ts–C27 18α(H)-22, 29, 30-trinorhopane; Tm–C27 17α(H)-22, 29, 30-trinorhopane; G–gammacerane; Tet–tetracyclic terpane; P–pregnane; HP–homopregnane; RS–regular sterane; TAS–triaromatic steroids.

biomarkers of crude oils from Group A and Group B are lower than that from Group C. The ratios of C_{29} 25-NH/C_{30}H (<1) and the ratios of C_{22} 17-NT/C_{23}TT (<0.1) from Group A and Group B crude oils are very low, reflecting that the biodegradation level of most of crude oils from Group A and Group B are still at the PM<7 stage. The biodegradation level of most of crude oils from Group C have reached the stage of PM>7, and the ratios of C_{29} 25-NH/C_{30}H (>1) and the ratios of C_{22} 17-NT/C_{23}TT (>0.5) are high. Among them, the ratio of C_{29} 25-NH/C_{30}H in Well 601-Incline 426 is as high as 16.57, and the value of C_{22} 17-NT/C_{23}TT is also as high as 1.38, which is the highest biodegradation level in the study area.

4.4. Carbon isotope composition characteristics of whole oil and oil bulk compositions

Stable carbon isotope of sedimentary organic matter is not only related to the source of organisms but also the environmental conditions and later evolution (Wang ZY et al., 2023). Carbon isotope composition of petroleum hydrocarbon

Table 3. Biodegradation biomarker parameters of Neogene Shawan Formation in the Chepaizi Uplift.

Position	Well	PM≥2	PM 1			PM≥5	PM≥6			PM≥7	PM≥8		PM≥9	
		a	b	c	d	e	f	g	h	i	j	k	l	m
Group A	C27	2.69	0.24	0.11	2.33	1.68	0.28	0.05	0.23	0.10	1.7	0.03	0.07	0.06
	C32	2.66	0.25	0.10	2.58	1.65	0.29	0.05	0.25	0.10	1.96	0.03	0.08	0.07
	C27-1	2.69	0.24	0.11	2.20	1.68	0.16	0.06	0.24	0.10	0.91	0.03	0.07	0.06
	P2-86	2.58	0.18	0.10	2.00	1.63	0.28	0.06	0.28	0.32	1.94	0.04	0.08	0.07
	P206	5.21	0.21	0.11	1.92	1.76	0.25	0.03	0.22	0.01	2.06	0.08	0.13	0.12
	P2-18	4.66	0.18	0.10	1.91	1.63	0.22	0.03	0.34	0.01	1.79	0.07	0.17	0.15
	C2-p41	4.64	0.25	0.11	2.36	1.61	0.22	0.04	0.21	0.01	2.23	0.07	0.13	0.11
	P8-p1	3.55	0.21	0.09	2.43	1.58	0.23	0.03	0.23	0.01	3.9	0.07	0.15	0.13
	P8-c3	3.91	0.26	0.10	2.62	1.59	0.23	0.03	0.31	0.01	3.57	0.06	0.13	0.12
	P2-p87	2.43	0.19	0.12	1.70	1.58	0.31	0.06	0.31	0.32	2.04	0.04	0.09	0.08
	P2-40	4.23	0.18	0.09	2.20	1.61	0.20	0.03	0.33	0.04	1.83	0.22	0.15	0.14
Group B	P2-88	3.27	0.53	0.17	2.95	1.19	0.36	0.17	0.08	0.32	1.69	0.04	0.17	0.19
	C2-p1	2.17	0.58	0.41	1.23	1.48	0.34	0.23	0.11	0.42	1.99	0.06	0.13	0.16
	C2-p2	1.77	0.25	0.40	0.44	1.19	0.37	0.19	0.12	0.42	3.05	0.06	0.11	0.12
	C26	1.87	1.73	0.80	2.40	1.34	0.56	0.07	0.08	0.12	2.71	0.06	0.15	0.17
	P2-93	3.08	0.42	0.18	2.04	1.21	0.28	0.17	0.11	0.32	4.48	0.04	0.17	0.15
Group C	P601-20	n.d.	n.d.	n.d.	n.d.	1.41	0.24	1.33	0.69	2.21	0.96	0.65	0.03	0.05
	P601-23	n.d.	n.d.	n.d.	n.d.	1.69	0.42	2.24	1.23	2.21	0.84	0.65	0.02	0.03
	P601-p119	n.d.	n.d.	n.d.	n.d.	1.10	0.71	0.61	0.10	2.21	2.13	0.65	0.03	0.05
	P601-p215	n.d.	n.d.	n.d.	n.d.	1.36	0.42	2.65	0.85	2.45	4.87	0.19	0.03	0.06
	P629	n.d.	n.d.	n.d.	n.d.	1.84	0.57	0.64	1.60	2.21	1.59	0.65	0.02	0.03
	P6-p21	0.00	0.00	0.00	0.00	3.51	0.73	0.89	0.55	2.21	2.52	0.65	0.07	0.08
	P601-x426	3.44	0.22	0.10	n.d.	1.36	0.54	2.65	0.85	16.57	4.87	1.38	0.03	0.06

Notes: a–(nC_{21} + nC_{22})/(nC_{28} + nC_{29}); b–Pr/nC_{17}; c–Ph/nC_{18}; d–Pr/Ph; e–TeBR; f–C_{27} DS/C_{27} RS; g–C_{23} TT/C_{30} H; h–G/C_{30} H; i–C_{29} 25-NH/C_{30} H; j–C_{27} DS βα/αβ; k–C_{22} 17-NT/C_{23} TT; l–C_{20} TAS/C_{28} TAS; m–C_{21} TAS/C_{28} TAS; n.d.–not determined due to the substantial removal of n-alkanes during biodegradation.

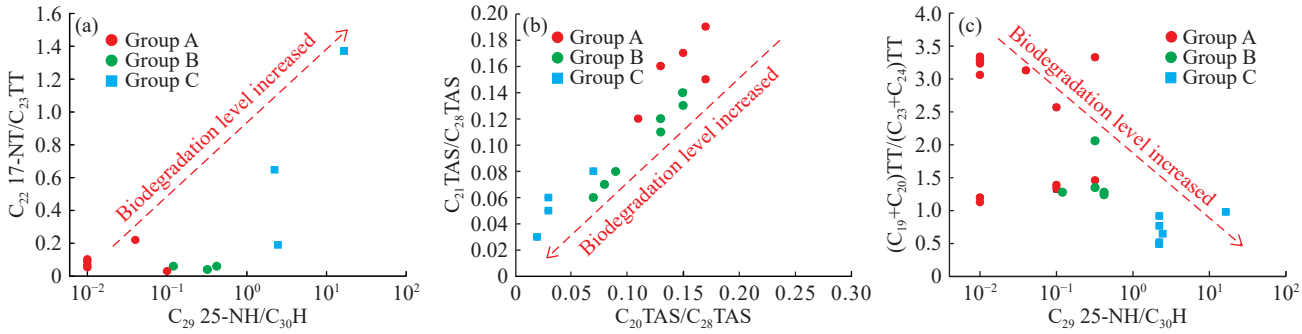

Fig. 7. Biodegradation level scatter plots of Neogene crude oils. a–Cross-plots of C_{29} 25-NH/C_{30}H *vs.* C_{22} 17-NT/C_{23}TT; b–C_{20}TAS/C_{28}TAS *vs.* C_{21}TAS/C_{28}TAS; c–C_{29} 25-NH/C_{30}H *vs.* (C_{19}+C_{20})TT/(C_{23}+C_{24})TT. NH–norhopane; H–hopane; NT–nortricyclic terpane; TT–tricyclic terpanes; TAS–triaromatic steroids.

inherits the organic matter composition of their parent rocks and is also influenced by the isotopic fractionation effect during the thermal maturation process to some extent. Peters KE and Moldowan JM (1993) believed that the stable carbon isotope (δ^{13}C) value does not change significantly with the change of biodegradation, but is greatly affected by the original composition of organic matter. In addition, due to the influence of maturity, the differences in the δ^{13}C values of crude oils from the same source rocks are usually no more than 1‰, while the differences in the δ^{13}C values of crude oils from different source rocks are usually 2‰–3‰ (Chung HM et al., 1992; Mao LX et al., 2020; Chang XC et al., 2022; Wang ZY et al., 2023).

Organic matter from higher plants exhibits relatively high δ^{13}C (−28.0‰ to −23.0‰), while organic matter from lower hydrobionts, algae and plankton have a relatively low δ^{13}C (−32.0‰ to −28.0‰) (Tissot BP and Welte DH, 1984).

δ^{13}C of whole oil, saturated hydrocarbon, and aromatics all become light from Group A, Group B to Group C (Fig. 8a; Table 4). Among them, the δ^{13}C of whole oil from Group A crude oils are mainly distributed at −27.4‰ to −26.6‰ (with an average of −27.21‰), and the δ^{13}C of saturated hydrocarbon are mainly distributed at −27.9‰ to −27.2‰ (with an average of −27.46‰). The δ^{13}C of aromatics range from −26.9‰ to −25.2‰ (with an average of −25.76‰). The δ^{13}C of Group B crude oils are mainly distributed in −28.8‰ to −27.0‰ (with an average of −27.84‰), and that of saturated hydrocarbon are mainly distributed in −29.7‰ to

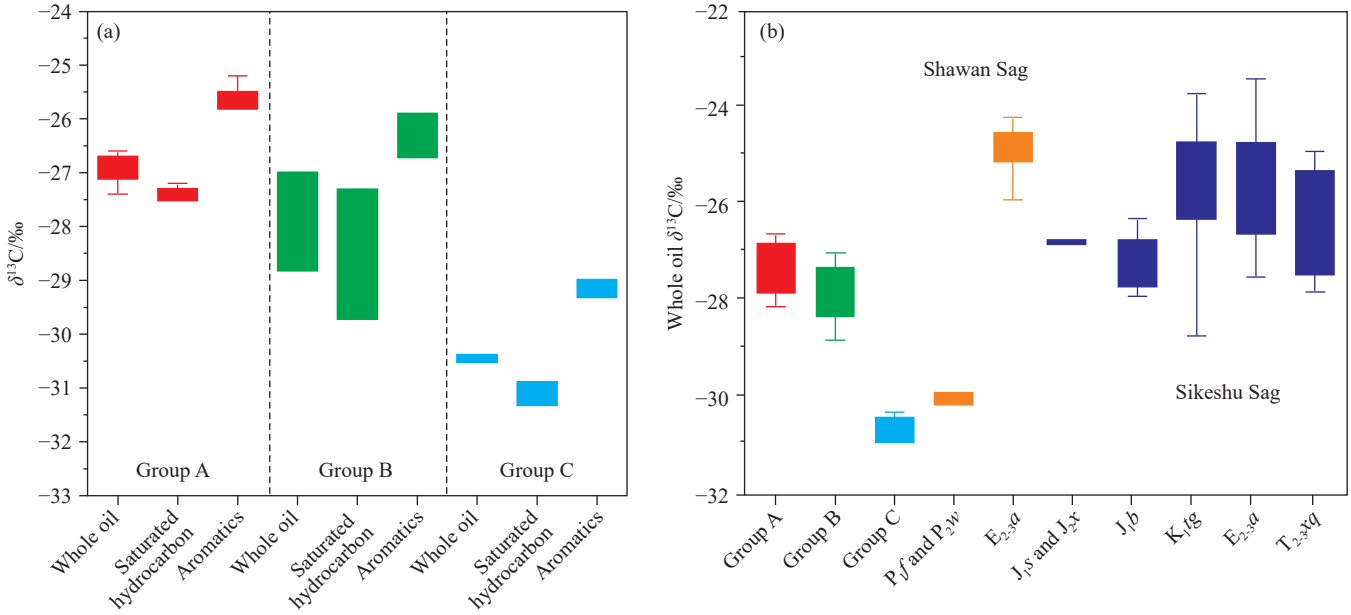

Fig. 8. a–Stock chart showing the distribution of stable carbon isotope of Neogene crude oil populations, and b–characteristics of whole oil stable carbon isotope. Group A–light oils occurred mainly in lower structure Neogene Shawan Formation in the western Chepaizi Uplift; Group B–heavy oils occurred mainly in higher structure Neogene Shawan Formation in the western Chepaizi Uplift; Group C–heavy oils occurred mainly in Neogene Shawan Formation in the eastern Chepaizi Uplift; P_1f and P_2w–source rocks of Permian; $E_{2\text{-}3}a$–source rocks of Paleogene Anjihaihe Formation; J_1s and J_2x–source rocks of Jurassic Sangonghe and Xishanyao Formation; J_1b–source rocks of Jurassic Badaowan Formation; K_1tg–source rocks of Cretaceous; $T_{2\text{-}3}xq$–source rocks of Triassic.

Table 4. Carbon isotope parameters of whole oil and oil bulk compositions from Neogene Shawan Formation in the Chepaizi Uplift.

Position	Well	Whole oil/‰	Saturated hydrocarbon/‰	Aromatics/‰	Non-hydrocarbon/‰	Asphaltene/‰
Group A	C2-p41	−26.70	−27.50	−25.80	−26.40	−27.30
	P206	−26.80	−27.40	−25.70	−26.20	−27.10
	P2−18	−26.80	−27.40	−25.50	−26.10	−27.10
	P2−40	−26.80	−27.30	−25.70	/	/
	C27	−27.40	−27.90	−26.90	−27.50	−27.50
	P8−c3	−26.60	−27.50	−25.50	−26.30	−27.10
	P8−p1	−27.10	−27.20	−25.20	−26.30	−27.20
Group B	C26	−27.00	−27.30	−25.90	−26.30	−27.10
	C2−p2	−28.80	−29.70	−26.70	−27.20	−27.70
	P2−93	−27.80	−28.40	−26.40	−27.30	−27.80
Group C	P601−x426	−30.50	−31.30	−29.30	−29.50	−29.50
	P6−p21	−30.40	−30.90	−29.00	−29.20	−29.20

−27.3‰ (with an average of −28.47‰). The $\delta^{13}C$ of aromatic hydrocarbon range from −26.7‰ to −25.9‰ (with an average of −26.33‰). The $\delta^{13}C$ of Group C crude oils are −30.9‰ to −30.3‰ (with an average of −30.57‰), and that of saturated hydrocarbon varied from −31.3‰ to −30.9‰ (with an average of −31.1‰). The $\delta^{13}C$ of aromatic hydrocarbon mainly range from −29.3‰ to −29.0‰ (with an average value of −29.15‰). This indicates that Group A and Group B are derived from a mixed input of large terrestrial organic matter and a small amount of aquatic algae or plankton, while Group C is derived from come from bacteria and algae in the lacustrine environment.

As shown in Fig. 8b and Table 4, the stable carbon isotope values of Group A and Group B crude oils are relatively heavy, which are well correlated with the source rocks in the Jurassic (J_2x, J_1b and J_1s), Paleogene ($E_{2\text{-}3}a$) and Triassic ($T_{2\text{-}3}xq$) in the Sikeshu Sag. The stable carbon isotope values of Group C crude oils are relatively light, which are in good contrast with the Permian (P_1f and P_2w) source rocks in the Shawan Sag. Due to the similar distribution of isotope values, it is difficult to distinguish the source of Group A and Group B crude oils solely based on carbon isotopes. Further analysis is needed in conjunction with the biomarker characteristics.

4.5. Biomarkers characteristics of Neogene crude oils

Group A and Group B crude oils from the western Chepaizi Uplift are dominated by $C_{19\text{–}20}TT$, indicating the input from large higher plants in peat swamps and small amount of aquatic algae or plankton, while Group C crude oils from the eastern Chepaizi Uplift are dominated by $C_{23}TT$, showing that the source of bacteria and algae are mainly in the lacustrine environment (Fig. 9a). Enriched C_{29} steranes generally represent higher contributions from higher plants,

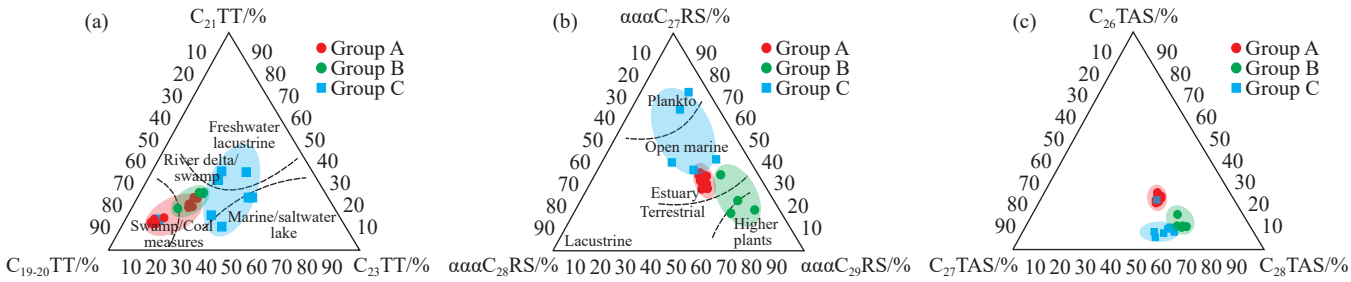

Fig. 9. a–Ternary plots of relative contents of $C_{19–20}$–C_{21}–C_{23}TT; b–αααC_{27}–C_{28}–C_{29}RS; c–C_{26}–C_{27}–C_{28}TAS. TT–tricyclic terpanes; RS–regular sterane; TAS–triaromatic steroids.

while abundant C_{28} steranes indicate the source of lake algae, and C_{27} steranes indicate the input of marine phytoplankton (Huang WY and Meinschein WG, 1979; Schwangler M et al., 2020). The tri-diagram of αααC_{27}–C_{28}–C_{29} regular steranes (Fig. 9b) shows that Group A and Group B crude oils from the western Chepaizi Uplift exhibit high levels of C_{29}RS, small amount of C_{27}RS and moderate amount of C_{28}RS, indicating mixed input of large terrestrial organic matter and small amount of aquatic algae or plankton, while Group C crude oils from the eastern Chepaizi Uplift indicate the source of bacteria and algae in the lacustrine environment dominated by C_{27}RS. The tri-diagram of C_{26}–C_{27}–C_{28} triaromatic steroids further confirms this conclusion (Fig. 9c).

It is believed that the Jurassic source rocks in the Sikeshu Sag in the Chepaizi area are mainly imported by higher plants or coal, the Paleogene source rocks in the Sikeshu Sag in the Chepaizi area are dominated by lower organisms, while the Permian source rocks in the Shawan Sag are mainly lacustrine deposits dominated by plankton-bacteria algae (Zhang ZH et al., 2012). From this, it can be preliminarily concluded that Group A and Group B crude oils may come from the mixed origins of Jurassic source rocks and Paleogene source rocks in the Sikeshu Sag, while Group C crude oils may come from the Permian source rocks in the Shawan Sag.

In addition, the gammacerane index (G/C_{30}H) distribution of crude oils in Group A and Group B (0.08–0.34, average 0.22) is similar to that of the Paleogene and Jurassic source rocks (0.2–0.4) in the Sikeshu Sag (Shi BB et al., 2019), indicating that the crude oils in Group A and Group B may mainly come from the Paleogene and Jurassic source rocks in the Sikeshu Sag.

4.6. Biomarker recovery method for oil-source correlation

Due to the selective consumption of different types of compounds in crude oils by biodegradation, the commonly-used biomarker fingerprints may change, making it difficult to connect oil-oil and oil-source correlation, and to determine the maturity and genotype of crude oils (Shi BB et al., 2020b; Gong DY et al., 2021; Chang XC et al., 2022). However, if the relationship between the reactants and products of a compound can be discovered during biodegradation, the content of the compounds can be adjusted, allowing the relevant parameters to be updated, and true geochemical information can be obtained.

At present, it is known that the main biomarkers with genetic connections are hopanes, tricyclic terpanes, and C_{24}-tetracyclic terpanes. The degradation products of the above three biomarkers in severe and extreme biodegradation crude oils correspond to 25-NH, demethylated tricyclic terpanes, and demethylated tetracyclic terpanes respectively.

In general, C_{29} 25-NH is produced by removing one –CH_3 from C_{30} hopane (Alberdi M et al., 2001; Peters KE, 2000). Therefore, based on the principle of mass conservation, the absolute concentration of the original C_{30} hopane should be equal to the absolute concentration of the degraded residual C_{30} hopane+the newly generated C_{29} 25-NH+the mass of –CH_3. Similarly, C_{22} 17-ntricyclic terpane is produced by removing one –CH_3 from C_{23} tricyclic terpane (Peters KE, 2000; Alberdi M et al., 2001), so the absolute concentration of the original C_{23} tricyclic terpane should be equal to the absolute concentration of the degraded residual C_{23} tricyclic terpane+the mass of the newly generated C_{22} 17-ntricyclic terpane + the mass of –CH_3.

Since the molecular weight of the methyl group formed after biomarkers degradation of crude oils are much lower than that of the original biomarkers, Eq. 1 is modified to Eq. 2 for subsequent calculation.

$$M_n^* = M_n + M_{n-1} + M - methyl \quad (1)$$

$$M_n^* \approx M_n + M_{n-1} \quad (2)$$

In the formula, M_n^* represents the mass of the biomarker with n carbon atoms before biodegradation; M_n represents the remaining mass of the biomarker with n carbon atoms after biodegradation; M_{n-1} is the mass of the biomarker with n−1 carbon atoms after biodegradation. *M-methyl* indicates the mass of the methyl group removed from the biomarker.

It is well known that hopanes mainly reflect the input of bacteria, terpanes are not only exist in higher plants, but also exist in bacteria and algae (Peng S et al., 2002). In addition, some specific tricyclic terpanes represent typical input of terrestrial organic matter (C_{19}–C_{20}TT), as well as input of marine or lacustrine organic matter (C_{23}–C_{24}TT) (Liu ZQ et al., 2022). Tetracyclic terpanes have high thermal stability and resistance to extreme biodegradation, and their high contribution usually indicates organic matter input from terrestrial higher plants (Peters KE and Moldowan JK, 1993).

In this study, the author selectively restored the

parameters related to $C_{30}H$, C_{19}–$C_{26}TT$, and $C_{24}Tet$ in Group A, Group B, and Group C crude oils. Among them, $C_{30}H^*\approx C_{30}H+C_{29}25\text{-}NH$, C_{19}–$C_{26}TT^*\approx C_{19}$–$C_{26}TT+C_{18}$–$C_{25}TT$, $C_{24}Tet^*\approx C_{24}Tet+C_{23}DTet$.

Because carbon isotope can clearly distinguish the characteristics of different source rocks, and is basically not affected by biodegradation, so carbon isotope is the most effective correlation index. Peters KE and Moldowan JK (1993) believe that the $\delta^{13}C$ value does not change significantly with biodegradation, but is greatly influenced by the original composition of organic matter (Hu QY et al., 2016). In addition, due to the influence of maturity, the differences in the $\delta^{13}C$ values of crude oils from the same source rocks are usually no more than 1‰, while the differences in the $\delta^{13}C$ values of crude oils from the different source rocks are usually between 2‰ and 3‰ (Chung HM et al., 1992; Mao LX et al., 2020; Chang XC et al., 2022; Wang ZY et al., 2023). This article selects stable carbon isotope combined with recovered tricyclic terpanes, tetracyclic terpanes, and triaromatic steroids with resistance to extreme biodegradation compare the Neogene Shawan Formation crude oils in the Chapaizi Uplift.

From the Figs. 10a–d and Table 5, $C_{23}TT^*/C_{21}TT^*$, $C_{23}TT^*/C_{30}H^*$ of Group A and B crude oils are relatively low, and $C_{24}Tet^*/C_{26}TT^*$, $C_{30}H^*/C_{26}TT^*$ are relatively high, which are well correlated with the Jurassic Badaowan Formation source rocks (J_1b) in the Sikeshu Sag. $C_{23}TT^*/C_{21}TT^*$, $C_{23}TT^*/C_{30}H^*$ of Group C crude oils are relatively high, and $C_{24}Tet^*/C_{26}TT^*$, $C_{30}H^*/C_{26}TT^*$ are relatively low, corresponding to the Permian source rocks (P_1f and P_2w) in the Shawan Sag.

In addition, it is generally believed that the ratios of isomers with different carbon numbers (20S and 20R configurations) can effectively reflect the maturity and sedimentary environment (Mackenzie AS, 1984). The crossplot of $\delta^{13}C$ and $C_{26}/C_{28}TAS$ (20S) (Fig. 10e) and $\delta^{13}C$ and $C_{27}/C_{28}TAS$ (20R) (Fig. 10f) also proves the above view.

Overall, the carbon isotope characteristics and parameters

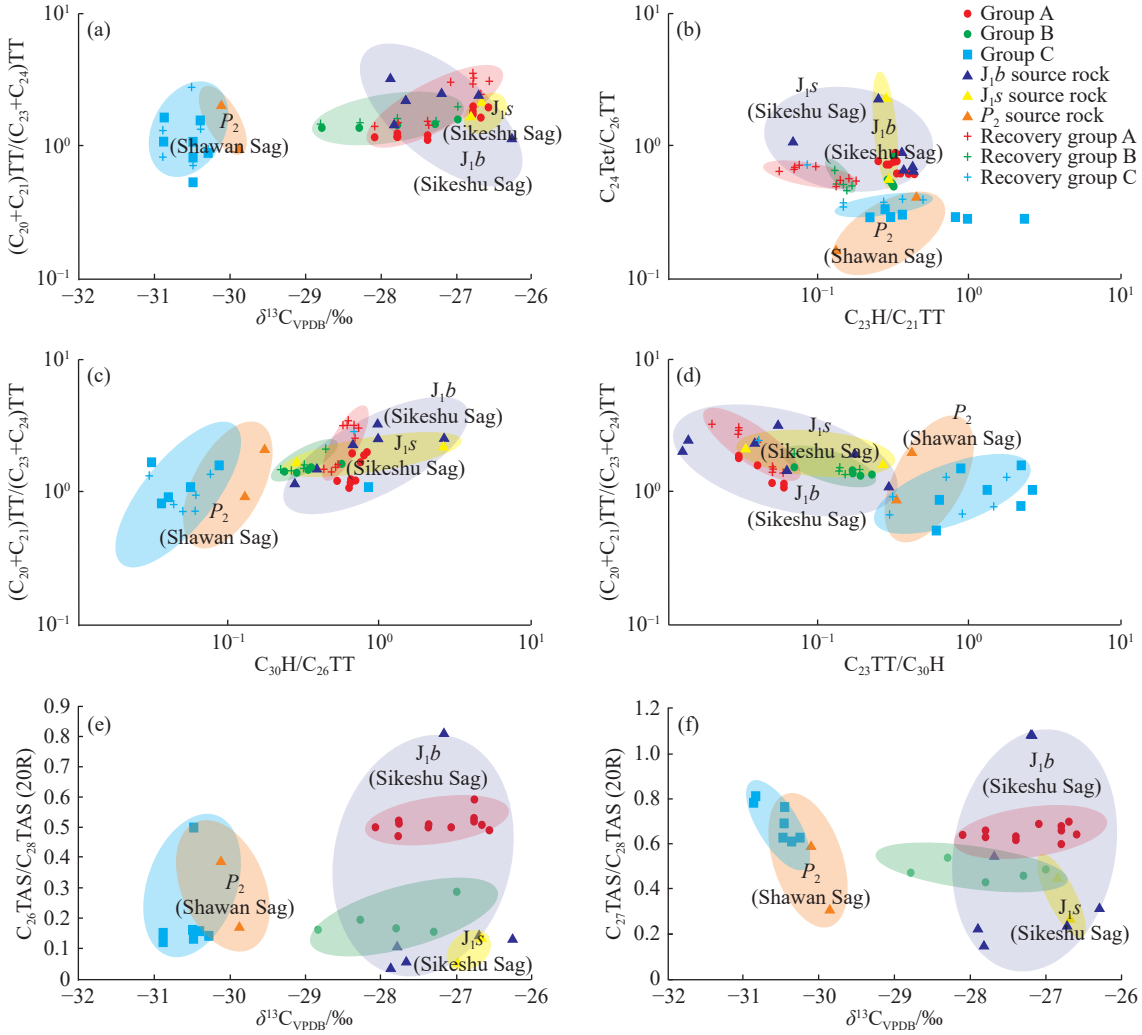

Fig. 10. Bivariate cross plots of oil-source correlation by biomarkers recovery method. a–cross-plots of $\delta^{13}C$ *vs.* $(C_{20}+C_{21})TT/(C_{23}+C_{24})TT$; b–$C_{23}H/C_{21}TT$ *vs.* $C_{24}Tet/C_{26}TT$; c–$C_{30}H/C_{26}TT$ *vs.* $(C_{20}+C_{21})TT/(C_{23}+C_{24})TT$; d–$C_{23}TT/C_{30}H$ *vs.* $(C_{20}+C_{21})TT/(C_{23}+C_{24})TT$; e–$\delta^{13}C$ *vs.* $C_{26}TAS/C_{28}TAS$; f–$\delta^{13}C$ *vs.* $C_{27}TAS/C_{28}TAS$. TT–tricyclic terpanes; Tet–tetracyclic terpanes; TAS–triaromatic steroids. *Notes*: The different shaded areas represent the projected areas of multiple-source rocks from Sikeshu and Shawan sag, as well as the projected areas before and after the recovery of three types of crude oils.

Table 5. Oil−source correlation parameters of Neogene Shawan Formation in the Chepaizi Uplift.

Position	Well	a	b	c	d	e	f	g	h	i	j	k	l	m
Group A	C27	1.20	−27.40	0.05	1.05	1.58	28.12	0.50	0.63	1.51	0.05	0.60	1.28	18.71
	C32	1.21	−27.80	0.05	1.13	1.50	26.32	0.52	0.63	1.54	0.05	0.61	1.26	19.17
	C27−1	1.11	−27.40	0.06	1.20	1.49	24.90	0.51	0.62	1.42	0.05	0.66	1.25	17.47
	P2−86	1.19	−27.80	0.06	0.93	1.90	19.24	0.47	0.66	1.45	0.05	0.54	1.10	14.67
	P206	1.85	−26.80	0.03	1.07	1.50	33.16	0.52	0.60	2.94	0.03	0.36	1.80	27.83
	P2−18	1.93	−26.80	0.03	0.97	2.04	26.01	0.53	0.68	3.09	0.03	0.35	1.68	23.48
	C2−p41	1.63	−26.70	0.04	1.03	1.50	31.03	0.51	0.70	2.45	0.04	0.44	1.81	27.04
	P8−p1	1.91	−27.10	0.03	0.83	2.08	25.87	0.50	0.69	3.02	0.03	0.35	1.65	22.01
	P8−c3	1.94	−26.60	0.03	0.99	2.59	35.51	0.49	0.64	3.08	0.03	0.37	1.87	27.19
	P2−p87	1.16	−28.10	0.06	1.01	1.51	25.08	0.50	0.64	1.40	0.06	0.56	1.26	17.18
	P2−40	1.91	−26.80	0.03	0.90	1.90	26.06	0.59	0.66	3.33	0.02	0.30	1.59	24.09
Group B	P2−88	1.45	−27.30	0.17	0.95	1.17	10.60	0.16	0.46	1.49	0.14	0.58	1.14	9.49
	C2−p1	1.40	−28.30	0.23	0.96	0.94	6.61	0.19	0.54	1.44	0.19	0.60	0.96	6.10
	C2−p2	1.37	−28.80	0.19	0.97	1.07	8.42	0.17	0.47	1.41	0.16	0.62	1.04	7.59
	C26	1.58	−27.00	0.07	0.97	2.34	21.14	0.29	0.49	1.99	0.07	0.53	1.66	15.23
	P2−93	1.50	−27.80	0.17	0.91	1.28	11.34	0.17	0.43	1.57	0.14	0.54	1.16	9.84
Group C	P601−20	1.07	−30.90	1.33	1.06	0.51	0.97	0.15	0.82	0.80	1.47	0.88	0.70	0.69
	P601−23	1.63	−30.90	2.24	0.76	0.46	0.44	0.12	0.77	1.31	1.80	0.58	0.69	0.42
	P601−p119	0.53	−30.50	0.61	3.71	0.46	0.91	0.13	0.77	0.70	0.30	1.31	0.76	1.04
	P601−p215	0.81	−30.50	2.22	1.83	0.48	0.54	0.16	0.62	0.71	0.91	1.08	0.77	0.83
	P629	0.90	−30.30	0.64	2.07	0.46	0.62	0.14	0.63	0.94	0.32	0.87	0.69	1.08
	P6−p21	1.55	−30.40	0.89	0.89	0.59	1.74	0.16	0.61	1.33	0.71	0.58	0.78	1.46
	P601−x426	1.07	−30.50	2.65	0.94	0.48	36.52	0.51	0.69	2.76	0.03	0.40	1.90	27.12

Notes: a–(nC_{20} + nC_{21}) TT/(nC_{23} + nC_{24}) TT; b–δ^{13}C/‰; c–C_{23} TT/C_{30} H; d–C_{23} TT/C_{21} TT; e–C_{24} Tet/C_{26} TT; f–C_{30} H/C_{26} TT; g–C_{26} TAS/C_{28} TAS(20R); h–C_{27} TAS/C_{28} TAS(20R); i–(nC_{20} + nC_{21}) TT*/(nC_{23} + nC_{24}) TT*; j–C_{23} TT*/C_{30} H*; k–C_{23} TT*/C_{21} TT*; l–C_{24} Tet*/C_{26} TT*; m–C_{30} H*/C_{26} TT*.

characteristics related to triaromatic steroids, which are consistent with the oil-source correlation results obtained by the biomarker recovery method, indicating that the biomarker recovery method is reliable for the oil-source correlation results of biodegradable crude oil. However, well P601-x426 in Group C, C_{23}TT*/C_{21}TT*, C_{23}TT*/C_{30}H* are relatively low, and C_{24}Tet*/C_{26}TT*, C_{30}H*/C_{26}TT* are relatively high, showing different characteristics to Group C crude oils. This may be due to its extreme biodegradation effect, which leads to significant loss of tricyclic terpanes.

4.7. Exploration potential of biomarker recovery methods

Biodegradation often alters the original characteristics of biomarkers, thereby limiting the identification of heavy oil sources. The biomarker recovery method is based on the principle of mass conservation, using the sum of the mass of the residual biomarkers and their corresponding degradation products to obtain the mass of the original biomarkers. It can restore the original biomarker characteristics of heavy oils, making it possible to determine the source of heavy oils using traditional and important biomarker parameters. Due to its low experimental cost and the presence of selected compounds in most crude oils, this method has a wider applicability in heavy oil source research than other methods. Based on the results of the application of this in severely to extremely biodegradable oils, research has shown that the biomarker recovery method has high resolution and potential application prospects in oil-source correlation, especially in severely to extremely biodegradable oils. It can support furthering oil and gas exploration in biodegradable areas and provide certain guidance for it. After the identification of oil and gas sources, the advantageous migration direction and migration path of oil and gas can also be roughly determined, so that it can know the enriched areas of oil and gas on the migration path, and guide the excavation of oil and gas exploration wells.

5. Conclusions

(i) The Chepaizi Uplift of the Junggar Basin (NW China) is adjacent to the two hydrocarbon-generating centers of Sikeshu Sag and the Shawan Sag. It possesses multiple sets of hydrocarbon-generating sags and multiple sets of potential source rocks. Moreover, the crude oils in this area have undergone intense biodegradation.

(ii) By using the biomarker recovery method and selecting parameters such as tricyclic terpanes, tetracyclic terpanes, triaromatic steroids, stable carbon isotopes, and others, in combination with the nature and occurrence of the crude oils in this area, the crude oils in this area can be classified into three groups, Group A, Group B, and Group C. Group A crude oils mainly exist in lower structure Neogene Shawan Formation in the western Chepaizi Uplift, while Group B crude oils mainly exist in higher structure Neogene Shawan Formation in the western Chepaizi Uplift. Both types of crude oils have higher $C_{19–20}$TT, higher C_{29}RS content, and heavier stable carbon isotopes, indicating that mixed input of large terrestrial organic matter and a small amount of aquatic algae or plankton in peat bogs. Group C crude oils mainly exist in

Neogene Shawan Formation in the eastern Chepaizi Uplift, showing enrichment of C_{23}TT; steranes are dominated by C_{27} steranes, and light stable carbon isotope, which are characterized by a brackish water lacustrine sedimentary environment.

(iii) The biomarker recovery method, based on the law of mass conservation, plays a positive role in the comparative identification of biodegraded crude oils and potential source rocks. After parameter recovery, parameters related to hopanes and tricyclic terpanes are more reliable, and the aggregation characteristics are more pronounced. The predicted results of recovered biomarkers are significantly different from those of the original parameters and are closer to the characteristic values of potential source rocks.

(iv) The oil-oil and oil-source correlations of Neogene Shawan Formation crude oils using the biomarker recovery method reveal that Group A and Group B crude oils have similar sources and come from the mixed source of Jurassic Badaowan Formation source rocks (J_1b) and Paleogene Anjihaihe Formation source rocks ($E_{2\text{-}3}a$) in the Sikeshu Sag, and Jurassic Badaowan Formation source rocks (J_1b) are the main source of crude oils. Group C crude oils are derived from Permian (P_1f and P_2w) source rocks in the Shawan Sag. Simultaneously, effective biomarker parameters and stable carbon isotopes further support this study and yield consistent results, indicating that biomarker recovery method has high resolution and potential application prospects in oil-source correlation, especially for severely to extremely biodegraded oils.

CRediT authorship contribution statement

Chen-Yu Wang, Xiang-Chun Chang conceived of the presented idea. Chen-Yu Wang carried out the experiment. All authors discussed the results and contributed to the final manuscript.

Declaration of competing interest

The authors declare no conflicts of interest.

Acknowledgments

This study was co-funded by the National Natural Science Foundation of China (42372160, 42072172). The authors thank the Shengli Oil Company of Sinopec for approving the publication. The authors are also grateful for the critical comments and helpful suggestions raised by two anonymous reviewers, who greatly improved the quality of our early version.

References

Alberdi M, Moldowan JM, Peters KE, Dahl JE. 2001. Stereoselective biodegradation of tricyclic terpanes in heavy oils from the Bolivar Coastal Fields, Venezuela. Organic Geochemistry, 32(1), 181–191. doi: 10.1016/s0146-6380(00)00130-3.

Chang XC, Zhao HG, He WX, Xu YH, Xu YD, Wang Y. 2018. Improved understanding of the alteration of molecular compositions by severe to extreme biodegradation: A case study from the Carboniferous oils in the eastern chepaizi uplift, Junggar basin, northwest China. Energy & Fuels, 32(7), 7557–7568. doi: 10.1021/acs.energyfuels.8b01557.

Chang XC, Wang Y, Shi BB, Xu YD. 2019. Charging of Carboniferous volcanic reservoirs in the eastern Chepaizi uplift, Junggar Basin (northwestern China) constrained by oil geochemistry and fluid inclusion. AAPG Bulletin, 103(7), 1625–1652. doi: 10.1306/12171818041.

Chang XC, Ge TC, Shi BB, Liu ZQ, Xu YD, Wang Y. 2022. Application of biomarker recovery method for oil–source correlation in severe to extreme biodegradation in eastern Chepaizi Uplift, Junggar Basin (NW China). Energy Reports, 8, 11865–11884. doi: 10.1016/j.egyr.2022.09.017.

Cheng X, Hou DJ, Xu CG, Wang FL. 2016. Biodegradation of tricyclic terpanes in crude oils from the Bohai Bay Basin. Organic Geochemistry, 101, 11–21. doi: 10.1016/j.orggeochem.2016.08.007.

Chung HM, Rooncy MA, Toon MB, Claypool GE. 1992. Carbon isotope composition of marine crude oils. American Association of Petroleum Geologists Bulletin, 76(7), 1000–1007. doi: 10.1306/BDFF8952-1718-11D7-8645000102C1865D.

Curiale JA. 2008. Oil–source rock correlations–Limitations and recommendations. Organic Geochemistry, 39(8), 1150–1161. doi: 10.1016/j.orggeochem.2008.02.001.

Dong DW, Li L, Wang XL, Zhao L. 2015. Structural evolution and dislocation mechanism of western margin chepaizi uplift of Junggar basin. Journal of Jilin University (Earth Science Edition), 45(4), 1132–1141 (in Chinese with English abstract). doi: 10.13278/j.cnki.jjuese.201504116.

Dong YL, Zhang MY, Zhu XM, Jiang Q, Guo L, Wei MP. 2017. Seismic geomorphology and depositional system of delta and terminal fan: A case study of the Neogene Shawan Formation in the Chepaizi Uplift, Junggar Basin, China. Marine and Petroleum Geology, 83, 362–381. doi: 10.1016/j.marpetgeo.2016.10.006.

Gong DY, Wang XL, Zhou CM, Zheng ML, Jiang WL, Wu WA. 2021. Discovery of large-scale Carboniferous source rocks and natural gas exploration potential in the southeast of Junggar Basin. Acta Petrolei Sinica, 42(7), 836–852 (in Chinese with English abstract). doi: 10.7623/syxb202107002.

GB/T 18340.2–2010 Organic geochemical analysis method for geological samples–Part 2: Determination of organic carbon stable isotopic component–Isotopic mass spectrometry, 2010 (in Chinese).

GB/T 18340.5–2010 Organic geochemical analysis methods for geological samples–Part 5: Analysis of saturated hydrocarbons in rock extracts and crude oils–Gas chromatography, 2010 (in Chinese).

GB/T 18606–2017 The test method for biomarkers in sediment and crude oil by GC–MS, 2017 (in Chinese).

Guo MY, Wu LW, Hu Y, Wu ZC, Ni PB, Li J, Deng GB. 2018. Classification method of crude oil genesis based on geochemical spectrogram characteristics: A case study on the eastern slope area of Shijiutuo uplift in Bohai Oilfield. Mud Logging Engineering, 29(4), 49–54,101 (in Chinese with English abstract). doi: 10.3969/j.issn.1672-9803.2018.04.011.

Hu QY, Dong DW, Zhao L, Li L, Li X, Kong X. 2016. Tectonic evolutionary characteristics and their causes of chepaizi uplift in Junggar basin. Oil & Gas Geology, 37(4), 556–564 (in Chinese with English abstract). doi: 10.11743/ogg20160412.

Huang WY, Meinschein WG. 1979. Sterols as ecological indicators. Geochimica et Cosmochimica Acta, 43(5), 739–745. doi: 10.1016/0016-7037(79)90257-6.

Jin X, Lu YC, Lu L. 2007. Analysis of the Mesozoic-Cenozoic subsidence history in chepaizi area, Junggar basin. Offshore Oil, 27(3), 51–56 (in Chinese with English abstract). doi: 10.3969/j.issn.

1008-2336.2007.03.008.

Li ET, Jin J, Mi JL, He D, Wang M, Li J, Ma WY, Wang HJ. 2021. Analysis of crude oil sources in the Chepaizi area, Junggar Basin. Geochimica, 50(5), 492–502 (in Chinese with English abstract). doi: 10.19700/j.0379-1726.2021.05.005.

Li NX, Huang HP, Jiang WL, Wu T, Sun JJ. 2015. Biodegradation of 25-norhopanes in a Liaohe basin (NE China) oil reservoir. Organic Geochemistry, 78, 33–43. doi: 10.1016/j.orggeochem.2014.10.007.

Li Y, Wu CD, Zhang XC, Xie LH, Leng JX, Guan XT. 2021. Heavy minerals characteristics, U-Pb geochronology and provenance analysis of Neogene Shawan formation in chepaizi uplift, Junggar basin. Acta Scientiarum Naturalium Universitatis Pekinensis, 57(6), 1058–1070 (in Chinese with English abstract). doi: 10.13209/j.0479-8023.2021.080.

Li Z, Zhang LY, Shen ZM, Guo CQ. 2011. Source and migrating direction of light oil in Chepaizi Uplift, Junggar Basin. Petroleum Geology & Experiment, 33(4), 419–423,436 (in Chinese with English abstract). doi: 10.3969/j.issn.1001-6112.2011.04.017.

Liu HJ, Zhang ZH, Qin LM, Zhu L, Xi WJ. 2011. Accumulation mechanism of light oils in Chepaizi uplift belt of Junggar Basin. Journal of China University of Petroleum (Edition of Natural Science), 35(4), 34–40 (in Chinese with English abstract). doi: 10.3969/j.issn.1673-5005.2011.04.006.

Liu HL, Wang HY, Zhao GL, Li GZ. 2004. Application of coal bed methane stable carbon isotope in exploration of coal bed methane field. Journal of Xi'an University of Science and Technology, 24(4), 442–446 (in Chinese with English abstract). doi: 10.13800/j.cnki.xakjdxxb.2004.04.012.

Liu ZQ, Chang XC, Xu YD, Shi BB, Zeng ZP, Zhang PF. 2022. Depositional environment, age determination and source diagnose of oils from the western Chepaizi Uplift (Junggar Basin) constrained by molecular biomarkers. Journal of Petroleum Science and Engineering, 214, 110495. doi: 10.1016/j.petrol.2022.110495.

MacKenzie AS, MacKenzie AS. 1984. Applications of biological markers in petroleum geochemistry. Advances in Petroleum Geochemistry. Amsterdam: Elsevier, 115–214. doi: 10.1016/b978-0-12-032001-1.50008-0.

Mao LX, Chang XC, Xu YD, Shi BB, Gao DK. 2020. Geochemical characterization and possible hydrocarbon contribution of the Carboniferous interval natively developed in the Chepaizi Uplift of Junggar Basin, northwestern China. Energy Exploration & Exploitation, 38(3), 654–681. doi: 10.1177/0144598719892901.

Peng SL, Nan P, Zhong Y. 2002. Terpenoids in higher plants and their roles in ecosystems. Chinese Journal of Ecology, 21(3), 33–38 (in Chinese with English abstract).

Peters KE, Moldowan JM. 1993. The Biomarker Guide: Interpreting Molecular Fossils in Petroleum and Ancient Sediments. New Jersey, Englewood Cliffs Nj Prentice Hall.

Peters KE. 2000. Petroleum tricyclic terpanes: Predicted physicochemical behavior from molecular mechanics calculations. Organic Geochemistry, 31(6), 497–507. doi: 10.1016/s0146-6380(00)00029-2.

Ren YZ. 2014. Geochemical characteristic of light hydrocarbon in crude oil, Shawan formation of Chepaizi uplift. Petroleum Geology and Recovery Efficiency, 21(3), 10–14,111 (in Chinese with English abstract). doi: 10.13673/j.cnki.cn37-1359/te.2014.03.004.

Schwangler M, Harris NB, Waldron JWF. 2020. Source rock characterization and oil-to-source rock correlation of a Cambrian-Ordovician fold-and-thrust belt petroleum system, western Newfoundland. Marine and Petroleum Geology, 115, 104283. doi: 10.1016/j.marpetgeo.2020.104283.

Shi BB, Chang XC, Yin W, Li Y, Mao LX. 2019. Quantitative evaluation model for tight sandstone reservoirs based on statistical methods - A case study of the Triassic Chang 8 tight sandstones, Zhenjing area, Ordos Basin, China. Journal of Petroleum Science and Engineering, 173, 601–616. doi: 10.1016/j.petrol.2018.10.035.

Shi BB, Chang XC, Xu YD, Mao LX, Zhang JH, Li Y. 2020a. Charging history and fluid evolution for the Carboniferous volcanic reservoirs in the western Chepaizi Uplift of Junggar Basin as determined by fluid inclusions and basin modelling. Geological Journal, 55(4), 2591–2614. doi: 10.1002/gj.3527.

Shi BB, Chang XC, Xu YD, Wang YR, Mao LX, Wang Y. 2020b. Origin and migration pathway of biodegraded oils pooled in multiple-reservoirs of the Chepaizi Uplift, Junggar Basin, NW China: Insights from geochemical characterization and chemometrics methods. Marine and Petroleum Geology, 122, 104655. doi: 10.1016/j.marpetgeo.2020.104655.

Song FQ, Ren DL, Zhang WL, Wang HT. 2004. GC-MS characteristics and oil source correlation of severely biodegradable crude oil. Journal of Instrumental Analysis, 23(S1), 304–305,308 (in Chinese).

Tissot BP, Welte DH. 1984. Geochemical fossils and their significance in petroleum formation. Petroleum Formation and Occurrence. Berlin, Heidelberg: Springer Berlin Heidelberg, 93–130. doi: 10.1007/978-3-642-87813-8_8.

Wang K, Ren XC, Lu WH, Ma K. 2017. Characteristics and hydrocarbon accumulation controlling factors of Neogene Shawan Formation reservoir in Chepaizi uplift, Junggar Basin. Geological Bulletin of China, 36(4), 547–554 (in Chinese with English abstract). doi: 10.3969/j.issn.1671-2552.2017.04.008.

Wang QJ, Chen L, Cao ZX, Zhang YJ, Shang FK, Ren XC. 2020. Hydrocarbon source analysis of light oil reservoirs in west wing of Chepaizi Uplift. Petroleum Geology and Recovery Efficiency, 27(4), 26–34 (in Chinese with English abstract). doi: 10.13673/j.cnki.cn37-1359/te.2020.04.003.

Wang ZY, Chang XC, Xu YD, Zhang PF, Shi BB, Ge TC, Yin YF, Su L. 2023. Origin of Mesozoic biodegraded crude oils from the eastern chepaizi uplift (Junggar basin) constrained by the biomarker recovery method. Energy & Fuels, 37(3), 1975–1997. doi: 10.1021/acs.energyfuels.2c03750.

Wenger LM, Davis CL, Isaksen GH. 2002. Multiple controls on petroleum biodegradation and impact on oil quality. SPE Reservoir Evaluation & Engineering, 5(5), 375–383. doi: 10.2118/80168-pa.

Xi WJ, Zhang ZH, Wang XZ. 2014. Oil source analysis and geochemical characteristics of heavy oil in Chunfeng Oilfield. Complex Hydrocarbon Reservoirs, 7(4), 19–23 (in Chinese with English abstract). doi: 10.16181/j.cnki.fzyqc.2014.04.005.

Xiao F, Liu LF, Wu KJ, Zhou CX, Xu ZJ, Deng SZ, Bai XY. 2015. Charging history of crude oils in the slope belt of the southern Junggar foreland basin, NW China: A case study from the east edge of chepaizi high. Energy Exploration & Exploitation, 33(5), 727–744. doi: 10.1260/0144-5987.33.5.727.

Xu YD, Chang XC, Shi BB, Wang Y, Li Y. 2018. Geochemistry of severely biodegraded oils in the Carboniferous volcanic reservoir of the Chepaizi Uplift, Junggar Basin, NW China. Energy Exploration & Exploitation, 36(6), 1461–1481. doi: 10.1177/0144598718770692.

Yang PC, Gao XZ, Ma J, Xiao JN. 2015. Oil source and hydrocarbon accumulation process in southwest of chepaizi uplift. Offshore Oil, 35(4), 13–19 (in Chinese with English abstract). doi: 10.3969/j.issn.1008-2336.2015.04.013.

You WF, Meng X L. 2006. Oil source analysis of well P-2 in the Chepaizi area of the Junggar Basin. West China Petroleum Geosciences, 2(1), 56–59 (in Chinese with English abstract).

Zhang BS, Li MJ, Zhao Q, Wang TG, Zhang K, Xiao ZY, Huang SY. 2016. Determining the relative abundance of C_{26}-C_{28} triaromatic steroids in crude oils and its application in petroleum geochemistry. Petroleum Geology & Experiment, 38(5), 692–697 (in Chinese with English abstract). doi: 10.11781/sysydz201605692.

Zhang WL, Zhang SN, Wang SQ. 2003. Geochemical characteristics of

oil and correlation of oil to resource rock in the southern edge of Junggar Basin. Journal of Chengdu University of Technology (Science and Technology Edition), 30(4), 374–377 (in Chinese with English abstract). doi: 10.3969/j.issn.1671-9727.2003.04.009.

Zhao XD, Zhang SQ, Yang SC, Ju XY, Chen GQ, Zhang XT, Khan D, Zhang YX, Zhang JK. 2021. Controlling factors of carbonate cement and its influence on oil-water distribution of the Neogene Shawan Formation in the northern Chepaizi area, Junggar Basin, NW China. Journal of Petroleum Science and Engineering, 206, 108942. doi: 10.1016/j.petrol.2021.108942.

Zhang XJ, Xu XY, Peng PA. 2013. Maturity assessment of light oils in Chepaizi Uplift and re-understanding of its source rock. Geochimica, 42(2), 180–187 (in Chinese with English abstract). doi: 10.19700/j.0379-1726.2013.02.008.

Zhang ZH, Li W, Meng XL, Qin LM, Zhang ZY, Yuan DS. 2007. Petroleum geochemistry and oil-source analysis in the southwest of chepaizi uplift, Junggar basin. Geoscience, 21(1), 133–140 (in Chinese with English abstract). doi: 10.3969/j.issn.1000-8527.2007.01.017.

Zhang ZH, Xiang K, Qin LM, Zhuang WS, Xi WJ, Zhao SF. 2012. Geochemical characteristics of source rocks and their contribution to petroleum accumulation of Chepaizi area in Sikeshu depression, Junggar Basin. Geology in China, 39(2), 326–337 (in Chinese with English abstract). doi: 10.3969/j.issn.1000-3657.2012.02.006.

Zhang ZH, Liu HJ, Li W, Fei JJ, Xiang K, Qin LM, Xi WJ, Zhu L. 2014. Origin and accumulation process of heavy oil in chepaizi area of Junggar basin. Journal of Earth Sciences and Environment, 36(2), 18–32 (in Chinese with English abstract). doi: 10.3969/j.issn.1672-6561.2014.02.005.

Zhang ZY, Zhu GY, Chi LX, Wang PJ, Zhou L, Li JF, Wu ZH. 2020. Discovery of the high-yield well GT1 in the deep strata of the southern margin of the Junggar Basin, China: Implications for liquid petroleum potential in deep assemblage. Journal of Petroleum Science and Engineering, 191, 107178. doi: 10.1016/j.petrol.2020.107178.

Zhuang XM. 2009. Petroleum geology features and prospecting targets of chepaizi uplift, Junggar basin. Xinjiang Geology, 27(1), 70–74 (in Chinese with English abstract). doi: 10.3969/j.issn.1000-8845.2009.01.016.